ENERGY, EXERGY AND EXERGOECONOMIC ANALYSIS OF A TRANS-CRITICAL CO_2 CYCLE POWERED BY A SINGLE FLASH GEOTHERMAL CYCLE IN WITH/WITHOUT ECONOMIZER WORKING MODES

Yashar ARYANFAR[1+], Soheil MOHTARAM[2**+], Humberto GARCIA CASTELLANOS[3], Elsayed M TAG-ELDIN[4], Busra ARSLA[5], Ahmed DEIFALLA[6], Adham E. RAGAB[7], HongGuang SUN[1*]

[1]State Key Laboratory of Hydrology-Water Recourses and Hydraulic Engineering, College of Mechanics and Materials, Hohai University, Nanjing 210098, Jiangsu, China.
[2]School of Energy and Power Engineering, University of Shanghai for Science and Technology, Shanghai 200093, China.
[3]Engineering Sciences, Tecnológico Nacional de México IT Ciudad Juárez, Juarez, Chihuahua, Mexico.
[4]Faculty of Engineering and Technology, Future University in Egypt New Cairo 11835, Egypt.
[5]Department of Energy Systems Engineering, Faculty of Technology, Gazi University, 06560, Technical Schools, Ankara, Türkiye.
[6]Future university in Egypt, 11835 Egypt.
[7]Department of Industrial Engineering, College of Engineering, King Saud University, P.O. Box 800, Riyadh 11421, Saudi Arabia.
[*] First corresponding author; E-mail: shg@hhu.edu.cn
[**] Second corresponding author; E-mail: S.mohtaram@usst.edu.cn
+ These authors contributed equally to this work and should be regarded as co-first authors.

The global utilization of renewable energy sources, particularly geothermal energy, is rising and the inefficient nature of geothermal cycles necessitates recovering lost heat. This research proposes a combined power generation cycle that simulates integrating a trans-critical carbon dioxide cycle with a single flash geothermal cycle, utilizing the EES. The study contrasts the system's performance between two operating states: "Without Economizer" and "With Economizer". The investigation analyzes the impact of an economizer on key output parameters, including energy efficiency, exergy efficiency, and net power output. In the "With Economizer" operating state, the net power output experiences a noticeable increase from 201.5 kW to 204.7 kW, resulting in a 1.58% enhancement in the performance of the "With Economizer" system. The energy efficiency metric demonstrates a corresponding improvement, rising by 1.55% from 3.28% in the "Without Economizer" system to 3.331% in the "With Economizer" system, aligning with the principles of the first law of thermodynamics. Furthermore, the energy efficiency, expressed as a percentage of energy units, shows an increase from 16.3% in the "Without Economizer" system to 16.56% in the "With Economizer" system, representing a 1.595% improvement based on the second law of thermodynamics or exergy. Regarding cost analysis, the study identifies the optimal separator pressure value for the system without an economizer, equivalent to 23. This configuration achieves a total cost rate of 01 $/GJ. Conversely, in the system with an economizer, the optimal pressure value for the production cost rate is 322.4 kPa, resulting in a cost rate of 23.57 $/GJ.

Key words*: Economizer, Production cost rate, Single flash Geothermal cycle, total cost rate, trans-critical CO_2 cycle*

1. Introduction

It's becoming increasingly evident that our planet's population is growing at an alarming rate. As a result, the demand for energy is skyrocketing every day [1]. It's crucial to acknowledge that fossil fuels are the primary source of energy for human activity worldwide. Nonetheless, it's worth noting that these sources are finite and pose a significant threat to the environment [2]. It's undeniable that the use of fossil fuels has had a devastating impact on our planet. We can see this through the melting of the polar ice caps and the threat to countless species. Not only that, but we've also seen an increase in natural disasters such as fires and storms that have caused irreversible damage. It's time to take action and make a change before it's too late. [3].

In contemporary times, there has been a notable emphasis on exploring alternative and environmentally friendly energy sources as a viable substitute for fossil fuels. This has led to a focus on renewable energy options like solar, wind, water, fuel cell, geothermal and biomass energies. [4]. Selecting an appropriate clean energy production approach is of utmost importance and requires careful consideration of various factors, including geographical and biological conditions, as well as operational expenses. Any energy conversion methods that may lead to environmental harm should be avoided, such as those that generate excess heat or discharge harmful pollutants. When it comes to selecting the ideal clean energy production method, it is essential to exercise caution and not take any unnecessary risks. [5]. In addition, energy conversion processes must be free of environmental hazards, and their adverse effects, such as the production of extreme heat and the release of environmental pollutants, must be avoided. Among the clean energy production methods, the use of wind and water energy has the lowest cost, and the use of solar power has the highest price. Geothermal energy is one of the best solutions for producing renewable energy because of various benefits. Geothermal energy may be utilized continuously, unlike other renewable sources of energy, which are constrained by certain seasons, times, and environmental factors [6]. Also, the cost of electricity in geothermal power plants is competitive with another standard (fossil) power plants and is even cheaper than different new energy types. Therefore, geothermal resources are significant due to their availability, simple technology for creating power plants, the possibility of uninterrupted operation and long-term use [7].

Using Engineering Equation Solver (EES) software, Huang et al. [8] proposed a power generation cycle combining a single flash geothermal cycle with a trans-critical carbon dioxide cycle. The results showed that the design features of the suggested system were significantly better than those of the BASIC single flash cycle. The Nelder-Mead simplex method and Genetic Algorithm were then used to refine the suggested strategy. A single flash geothermal cycle paired with a transcritical carbon dioxide recovery cycle is the geothermal power generation system, Wang et al. [9] suggested. A recuperator was employed to recover part of the heat loss to enhance system performance. Aryanfar et al. [10] investigates, simulates, and analyzes three operational modes of a newly constructed geothermal power plant. The initial mode was the single flash geothermal cycle (SFGC). An SFGC with two stages of organic Rankine cycles (ORC) recovery served as the second mode, while an SFGC with two stages of ORC recovery and LNG cryogenic energy served as the third. The ability of the N_2O, CO_2, and H_2O EGS to extract heat was compared by Liu et al. [11]. A two-dimensional thermo-hydraulic-mechanical (THM) coupled EGS model with discrete fractures is created. The effects of the

injection-production parameters on the heat extraction outcomes of the EGS employing various working fluids are also examined. The outcomes demonstrate that under the same circumstances, N_2O-EGS and CO_2-EGS perform almost equally in heat extraction. Sahana et al. [12] suggested employing a supercritical CO_2 power cycle to recover heat in the HWCS when hot water was delivered from the oilfield at a temperature close to 140 °C. The output of a supercritical CO_2 power cycle drives the compressor of an ejector expansion CO_2 refrigeration cycle. Using some of the CO_2 cycle reject heat, the HDH (Humidification-Dehumidification) desalination unit may produce fresh water. In a study, Wang et al. [13] used supercritical CO_2 (sCO_2) to simulate geothermal heat mining. The requirements for choosing the working fluid for ORCs that use sCO_2 from a geothermal reservoir are then given for subcritical, superheated, and supercritical ORCs. In the interim, a practical fluid classification method for ORC is being suggested. Models were utilized by Jiang et al. [14] to predict system efficiencies for standalone and hybrid systems. It has been found that the hybrid system has an efficiency that is on par with or even higher than the combined efficiency of the two individual CO_2-EGS and CO_2-solar thermal systems when compared to standalone CO_2-EGS and CO_2-solar thermal systems.

According to Liu et al. [15] research, the compression techniques used in supercritical CO_2 (S-CO_2) and transcritical CO_2 (T-CO_2) power cycles differ, and their implications for the equipment's and power cycles' thermodynamic performance are explored. According to the data, there is a significant gain in thermal efficiency and net output power close to the critical temperature and a decrease in compressor/pump inlet temperature overall. A recompression supercritical carbon dioxide Brayton cycle coupled with a solar power tower was proposed by Cao et al. [16]. Two energy storage stages are creatively used to increase the stability of the solar subsystem for continuous daily operation. Additionally, a solid oxide electrolyzer is included in the plan. Liu et al. [17] used both conventional and advanced exergy evaluations to evaluate the exergetic performance within the transcritical CO_2 ejector refrigeration system integrated with a thermoelectric sub-cooler (EJE + TES). The findings show that 89.44% of the total energy destruction is endogenous, which amply proves that there are no close relationships among the system's constituent parts.

This study focuses on a comparative analysis of a single flash geothermal cycle powered by a trans-critical carbon dioxide cycle, considering two operating modes: "Without Economizer" and "With Economizer". The systems are designed, and their thermodynamic behavior is modeled using EES software, incorporating thermodynamic equations and the first and second laws of thermodynamics. The main objective of this research is to investigate the impact of adding an economizer to the system, specifically analyzing its effects on energy efficiency, exergy efficiency, and net power output. Additionally, a comparative sensitivity analysis is conducted to assess the influence of critical parameters on the system's performance in both operating modes. The key aims of this study are as follows:

- Develop a comprehensive model of a single flash geothermal power plant utilizing a trans-critical CO_2 cycle, considering both "Without Economizer" and "With Economizer" operating modes.
- Conduct a comparative study between the two operating modes, assessing their respective performance and characteristics.
- Investigate the variations in energy efficiency, exergy efficiency, and net power output in response to changes in critical system parameters.

- Perform an economic analysis of the "Without Economizer" and "With Economizer" systems, including a sensitivity analysis of relevant economic parameters.

The proposed systems are implemented in the EES software, utilizing thermodynamic equations and primary data, to obtain output results for comparison. The subsequent sections present and discuss the changes in output parameters, such as energy efficiency, exergy efficiency, net power output, total cost rate, and production cost rate. Comparative diagrams are used to visualize and analyze these changes concerning variations in separator pressure, CO_2 turbine inlet pressure, and CO_2 condenser temperature for both operating modes.

2. Modeling and cycle description

The single-flash geothermal cycle driven by the trans-critical carbon dioxide cycle is shown in Fig.s 1(a) and 1(b) in "Without Economizer" and "With Economizer" working modes. Software called EES was used to simulate the system. In the simulation approach, each system component is employed as a control volume engineering, and the first and second laws of thermodynamics are applied to it.

During the decompression process, in which the pressure is reduced while maintaining a constant enthalpy, the geo-fluid that has entered the system is transformed into a two-phase fluid, as illustrated in Fig. 1(a). The steam turbine is powered by the two-phase fluid's saturated vapor component, which moves into the separator. The vapor generator (VG), which increases the temperature of carbon dioxide gas before the heat exchanger's outlet fluid is routed to the ground, also receives the saturated liquid component of the separator. It is delivered to the gas turbine at the proper pressure and temperature, producing more power for the entire system.

Figure 1(b) shows the installation of an economizer between the CO_2 pump and the VG to enhance system efficiency. The steam turbine's output stream (point 5) enters the economizer and warms the CO_2 pump's output stream before it reaches the condenser (point 9). Finding the congestion point in a trans-critical cycle is difficult because the temperature change's slope changes when carbon dioxide gas heats up within heat exchangers like an evaporator. The temperature difference between the beginning and the end is considered constant for ease of solution.

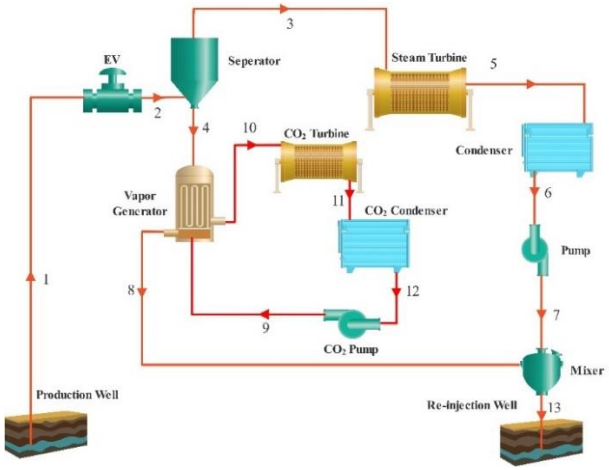

(a)

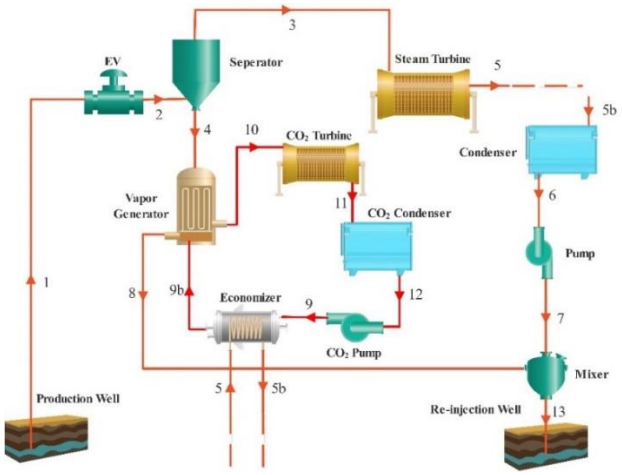

(b)

Fig. 1. Schematic of the proposed single flash geothermal cycle powered by a trans-critical CO_2 (a) Without Economizer (b) With Economizer.

EES is a comprehensive equation-solving software that can numerically solve thousands of coupled nonlinear algebraic and differential equations. This program can also solve differential equations and integrals, perform optimization, provide uncertainty analysis, perform linear and nonlinear regression, unit conversion and provide quality graphs. One of the main features of EES is a very accurate database of thermodynamic properties and transport properties, which is provided for hundreds of materials in a way that allows it to be used with the ability to solve the equation.

2.1. Governing equations

According to equations (1) and (2) and neglecting kinetic and potential energies, the system is written while considering the control volume, mass, and energy balances for each component of the system (2) [18-22]:

$$\sum \dot{m}_i = \sum \dot{m}_o \tag{1}$$

$$\sum \dot{Q} + \sum \dot{m}_i h_i = \sum \dot{m}_o h_o + \dot{W} \tag{2}$$

where $\dot{m}_i$ is the input flow rate and $\dot{m}_o$ is the output flow rate. Also, h_i is the enthalpy of the input flow, and h_o is the enthalpy of the output flow. $\dot{W}$ is the work and $\dot{Q}$ is the exchanged heat. Equations (3) and (4) will yield the isentropic efficiency and net power production of each turbine:

$$\eta_{Tur} = \frac{h_i - h_o}{h_i - h_{o,s}} \tag{3}$$

$$\dot{W}_{Tur} = \dot{m}_i(h_i - h_o) \tag{4}$$

The isentropic efficiency and net power of each pump are represented as follows:

$$\eta_{Pump} = \frac{h_i - h_{o,s}}{h_i - h_o} \tag{5}$$

$$\dot{W}_{Pump} = \dot{m}_i(h_o - h_i) \tag{6}$$

Equations (7), (8), and (9) will represent the net power of the system as well as the energy efficiency and exergy efficiency of the entire system [23-26]:

$$\dot{W}_{net} = \dot{W}_{tur,steam} + \dot{W}_{tur,CO2} - \dot{W}_{pump,steam} - \dot{W}_{pump,CO2} \quad (7)$$

$$\eta_{en} = \dot{W}_{net}/\dot{Q}_{in} \quad (8)$$

$$\eta_{ex} = \dot{W}_{net}/E_{in} \quad (9)$$

In the current investigation, the following hypotheses are considered [27-33]:

1. All cycle parts function in steady-state situations (as a control volume).
2. Changes in kinetic energy and potential in all components are insignificant, and pressure drop and heat loss in pipelines can be disregarded.
3. The isotropic efficiency of pumps is 0.75, while that of turbines is 0.8.
4. The ambient temperature and pressure for the analysis that is being presented are 25 °C and 0.1 MPa, respectively.

A cost rate balance for the entire system can be stated as below in the economic analysis [34]:

$$\dot{C}_{total} = \dot{C}_{fuel} + \sum_{k} (\dot{Z}_{CI} + \dot{Z}_{OM})_k \quad (10)$$

where $\dot{C}_{total}$ ($= c_{product}\dot{W}_{net}$) and $\dot{C}_{fuel}$($= c_G\dot{E}x_1$) stand for the respective total (or product) and fuel cost rates. Following are estimates for the total running, maintenance, and capital expenditure cost rates for each system component [35, 36]:

$$\dot{Z}_{CI,k} + \dot{Z}_{OM,k} = \frac{Z_k \times \emptyset}{N \times 3600} CRF \quad (11)$$

Z_k is the investment cost of each component, $\emptyset$ maintenance coefficient, N is the number of annual operating hours and *CRF* is the return on investment coefficient. According to the following expression, *CRF* can be calculated [35]:

$$CRF = \frac{i(i+1)^n}{(i+1)^n - 1} \quad (12)$$

So "*i*" is the interest rate and "*n*" is the useful life of the system. The investment cost function for each system component is displayed in Tab. 1.

Table 1. The investment cost function of different system components

Component	Capital Cost Function
Condenser	$1773 \times \dot{m}$ [37]
Economizer	$2143 \times (A_{Economizer})^{0.514}$ [38]
Pump	$1120 \times (\dot{W}_{pump})^{0.8}$ [34]
VG	$2143 \times (A_{VG})^{0.514}$ [38]
Steam Turbine	$6000 \times \dot{W}_T^{0.7}$ [37]
Gas Turbine	$\left(\frac{1536\dot{m}_{CO2}}{0.92-\eta_T}\right) \times \ln\left(\frac{P_i}{P_o}\right) \times [1 + exp(0.036T_i - 54.4)]$ [37]

Calculating certain factors in economic research, such as total cost, return on investment, and cost of producing an energy unit, might help to make the situation clearer.

$$\dot{C}_{tot} = c_{product}\dot{W}_{net} \quad (13)$$

That $\dot{C}_{tot}$ shows the total cost rate of the system and $c_{product}$ is product cost. Table 2(a) presents the essential data required for system simulation in the software environment. One of the main components of any application is the data it uses. Familiarity with data types in programming helps a lot to use them in the right place. This will improve the performance and speed of programming. Table 2(b) shows the validation of the present modeling by Wang's work. The amount of error is minimal, and therefore the validity of the modeling is confirmed.

Table 2(a). Initial data for modeling [23, 34, 39]

Definition	Values
Ambient temperature (T_0)	25 °C
Ambient Pressure (P_0)	100 kPa
Geothermal fluid inlet temperature (T_1)	170 °C
Geo-fluid mass flow rate ($\dot{m}_1$)	10 kg/s
Geo-fluid inlet pressure (P_1)	Saturated
Separator pressure (P_2)	500 kPa
Steam turbine output pressure (P_5)	20 kPa
CO_2 turbine inlet pressure (P_{10})	15000 kPa
CO_2 condenser temperature (T_{cond})	30 °C
Turbine isentropic efficiency (t_{urn})	0.8
Pump isentropic efficiency (η_{pump})	0.75
Evaporator inlet-outlet difference temperature (ΔT_{TTD})	20 °C
Heat Exchanger Pinch Point (ΔT_{PP})	5 °C
Annual operational hours the system (N)	7300 h
Annual interest rate (i)	14 %
Lifetime of the system (n)	15 years
Maintenance factor (∅)	1.06
Unit cost of exergy of the geothermal source (c_G)	1.3 $/GJ

Table 2(b). Validation of the current work outputs with [9]

Point	Working fluid	T (°C)		h (kJ/kg)		s (kJ/kg.K)	
		[9]	This work	[9]	This work	[9]	This work
1	Geo-fluid	170	170	719.3	719.1	2.042	2.042
2	Geo-fluid	151.9	151.8	719.3	719.1	2.047	2.046
3	Geo-fluid	151.9	151.8	2749	2748	6.821	6.821
4	Geo-fluid	151.9	151.8	640.4	640.1	1.861	1.86
5	Geo-fluid	60.07	60.06	2348	2347	7.122	7.122
6	Geo-fluid	60.07	60.06	251.5	251.4	0.8321	0.832
7	Geo-fluid	60.13	60.12	252.1	252.1	0.8326	0.8325

3. Results and discussions

In this section, the suggested systems' performance is assessed and analyzed, and the findings of the energy and exergy analyses are shown in tables and figures. The values of the input parameters are listed in Tab. 1 so that you can see how different parameters affect the system's performance. Temperature, pressure, mass flow rate, enthalpy, and entropy are the four thermodynamic parameters for the "Without Economizer" system in Tab. 3 and the "With Economizer" system in Tab. 4.

Table 3. Thermodynamic properties of the different points of the system in "Without Economizer" working mode.

State	Working Fluid	T (°C)	P (kPa)	h (kJ/kg)	s (kJ/kg.K)	$\dot{m}$ ($\frac{kg}{s}$)	x (-)	E (kW)
1	Geo-Fluid	170	791.5	719.3	2.042	10	-	1236
2	Geo-Fluid	151.9	500	719.3	2.047	10	0.03742	1223
3	Geo-Fluid	151.9	500	2749	6.821	0.3742	1	281.7
4	Geo-Fluid	151.9	500	640.4	1.861	9.626	0	941.1
5	Geo-Fluid	60.07	20	2348	7.122	0.3742	0.8891	98.55
6	Geo-Fluid	60.07	20	251.5	0.8321	0.3742	0	3.863
7	Geo-Fluid	60.13	500	252.1	0.8326	0.3742	-	4.053
8	Geo-Fluid	131.9	500	554.5	1.654	9.626	-	698.2
9	CO_2	52.1	15000	-186.3	-1.383	5.016	-	1104
10	CO_2	111.9	15000	-21.52	-0.9137	5.016	-	1240
11	CO_2	54.43	7214	-47.75	-0.8936	5.016	-	1079
12	CO_2	30	7214	-202.2	-1.395	5.016	0	1042
13	Geo-Fluid	129.2	500	543.2	1.626	10	-	694.3

Table 4. Thermodynamic properties of the different points of the system in "With Economizer" working mode.

State	Working Fluid	T (°C)	P (kPa)	h (kJ/kg)	s (kJ/kg.K)	$\dot{m}$ ($\frac{kg}{s}$)	x (-)	E (kW)
1	Geo-Fluid	170	791.5	719.3	2.042	10	-	1236
2	Geo-Fluid	151.9	500	719.3	2.047	10	0.03742	1223
3	Geo-Fluid	151.9	500	2749	6.821	0.3742	1	281.7
4	Geo-Fluid	151.9	500	640.4	1.861	9.626	0	941.1
5	Geo-Fluid	60.07	20	2348	7.122	0.3742	0.8891	98.55
5b	Geo-Fluid	60.07	20	1910	5.81	0.3742	0.7036	78.8
6	Geo-Fluid	60.07	20	251.5	0.8321	0.3742	0	3.863
7	Geo-Fluid	60.13	500	252.1	0.8326	0.3742	-	4.053
8	Geo-Fluid	72.1	500	302.2	0.9802	9.626	-	169.9
9	CO_2	52.1	15000	-186.3	-1.383	5.323	-	1171
9b	CO_2	55.07	15000	-176.8	-1.395	5.323	-	1176
10	CO_2	111.9	15000	-21.52	-0.9137	5.323	-	1316
11	CO_2	54.43	7214	-47.75	-0.8936	5.323	-	1145
12	CO_2	30	7214	-202.2	-1.395	5.323	0	1106
13	Geo-Fluid	129.2	500	543.2	1.626	10	-	694.3

Table 5 shows the output results from the simulation of systems in two "Without Economizer" and "With Economizer" working modes. One of the crucial points of Tab. 5 is the increase of the net power output from 201.5 kW to 204.7 kW, which indicates a 1.58 % increase in the "With Economizer" system. Regarding energy efficiency, this value is 3.28 % for the "Without Economizer" system and reaches 3.331 % in the "With Economizer" system, representing a 1.55 % improvement from the point of view of the first law of thermodynamics. In terms of exergy efficiency, the value of this efficiency for the "without economizer" system is 16.3 %. The "with economizer" system reaches 16.56 %, representing an improvement of 1.595 % from the point of view of the second law of thermodynamics or exergy.

Table 5. The output results from the simulation of systems in two "Without Economizer" and "With Economizer" working modes.

Parameters	Definition	"Without Economizer" operating mode	"With Economizer" operating mode	Units
$W_{tur,\ steam}$	Power production of the steam turbine	150.1	150.1	kW
$W_{tur,\ CO2}$	Power production of the CO_2 turbine	131.6	139.6	kW
$W_{pump,\ steam}$	Power consumption of steam pump	0.2436	0.2436	kW
$W_{pump,\ CO2}$	Power consumption of CO_2 pump	79.94	84.84	kW
W_{net}	Total net power output	201.5	204.7	kW
$\boldsymbol{\eta_{en}}$	Energy Efficiency	3.28	3.331	%
$\boldsymbol{\eta_{ex}}$	Exergy efficiency	16.3	16.56	%
$\boldsymbol{\dot{C}_{total}}$	Total cost rate	0.1406	0.1444	M$/Year
$\boldsymbol{C_{product}}$	Product cost rate	26.54	26.85	$/GJ

The findings of the study suggest that incorporating an economizer into a proposed system, which is a single flash geothermal system utilizing a trans-critical carbon dioxide cycle, results in a modest improvement of about 1.5% in the fundamental output parameters of the examined system. Energy efficiency, exergy efficiency, and net power output are graphed in Fig.s 2(a), (b), and (c) for both the "Without Economizer" and "With Economizer" modes of operation as it relates to separator pressure variation. The two systems exhibit similar behaviors as separator pressure increases from 150 kPa to 650 kPa. Graphs for all three parameters display an upward trend with increasing pressure, culminating in a peak value at approximately 250 kPa before experiencing a downward trend.

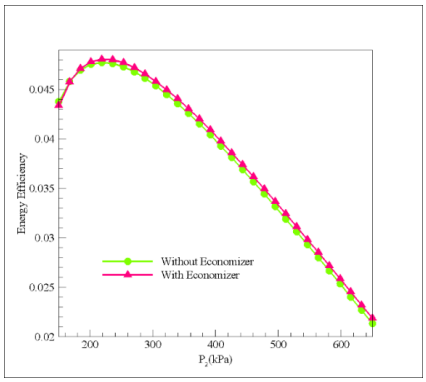

(a)

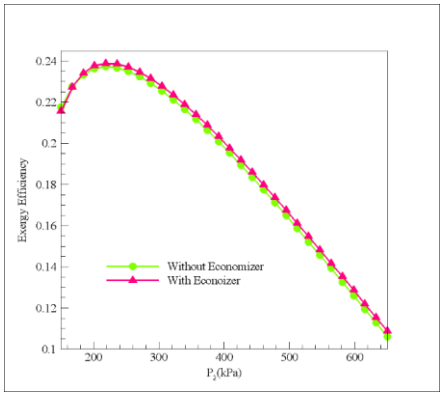

(b)

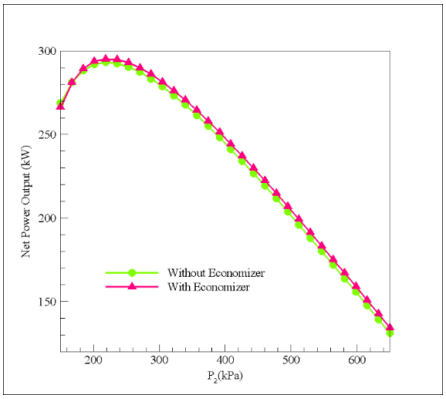

(c)

Fig 2. (a) Energy efficiency, (b) Exergy efficiency & (c) Net power output of the systems ("Without Economizer" and "With Economizer") variation with separator pressure.

Figures 3(a), (b) and (c) show the energy efficiency, exergy efficiency and net power output of the systems in "Without Economizer" and "With Economizer" working modes variation with CO_2 turbine inlet pressure, respectively. By increasing the inlet pressure of the CO_2 turbine from 14000 kPa to 16000 kPa, for the "Without Economizer" system, all three parameters of energy efficiency, exergy efficiency and net power output, the figures started an increasing trend, around 15000 kPa, to the maximum value. It reaches itself, and after that, they have a downward trend. But in the case of the " With Economizer" system, the behavior of the figures is different. With the increase of pressure from 14000 kPa to 16000 kPa, all three figures have a decreasing trend, which shows the negative effect of increasing the inlet pressure of the CO_2 turbine on the performance of the whole system.

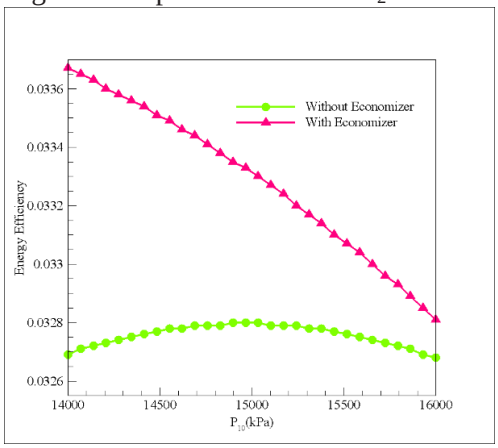

(a)

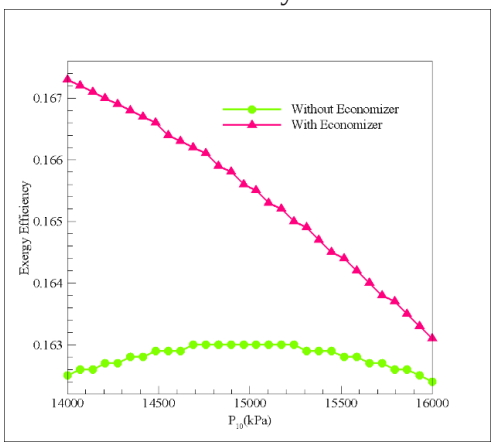

(b)

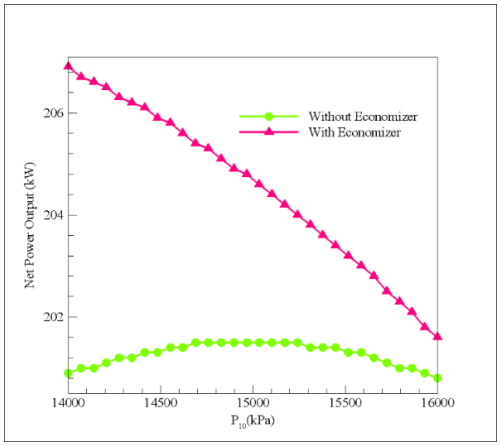

(c)

Fig. 3. (a) Energy efficiency, (b) Exergy efficiency & (c) Net power output of the systems ("Without Economizer" and "With Economizer") variation with CO2 turbine inlet pressure.

Figures 4(a), (b) and (c) show the energy efficiency, exergy efficiency and net power output of the systems in "Without Economizer" and "With Economizer" working modes variation with CO_2 condenser exit temperature, respectively. With the increase of temperature from 25 °C to 31 °C, all three figures have a decreasing trend, which shows the negative effect of increasing the CO_2 condenser exit temperature on the whole system's performance in both working modes. This situation is such that from around 30.6 °C, all three parameters of energy efficiency, exergy efficiency and net power output of the "With Economizer" system are equal to the "Without Economizer" system. These output parameters are lower than the "Without Economizer" system at higher temperatures.

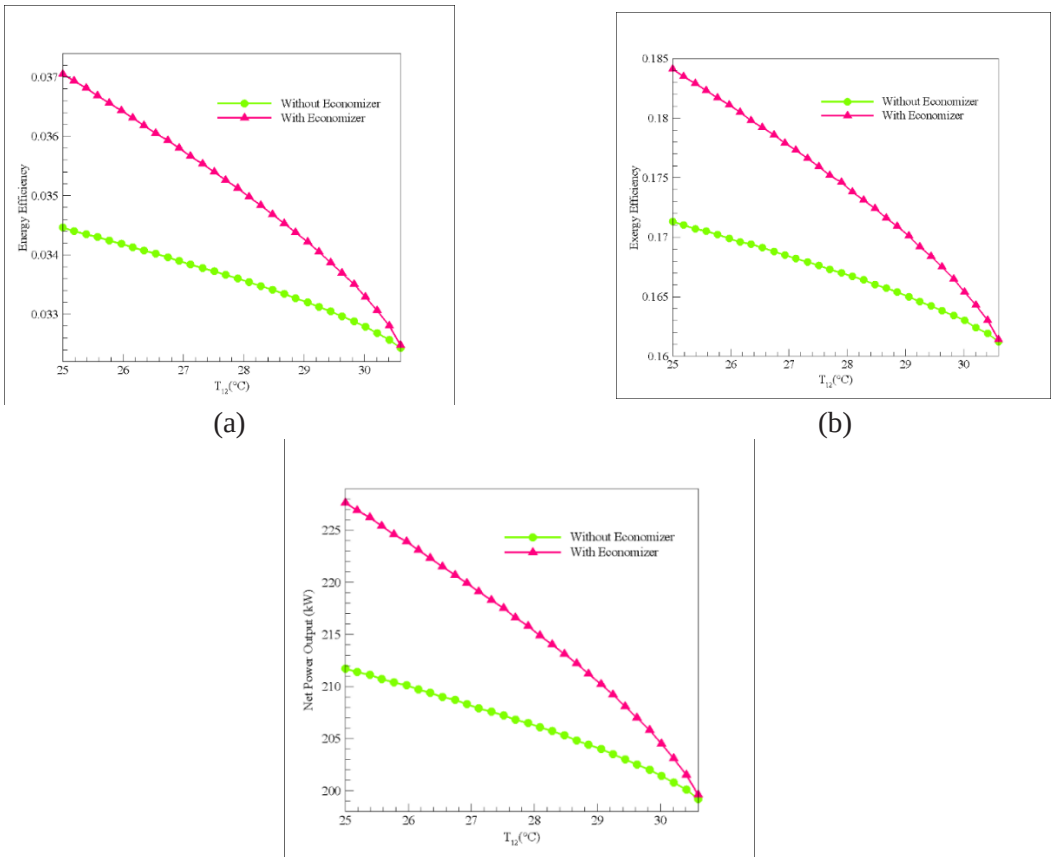

Fig 4. (a) Energy efficiency, (b) Exergy efficiency & (c) Net power output of the systems ("Without Economizer" and "With Economizer") variation with CO2 condenser exit temperature.

Figures 5(a) and (b) show the total cost rate and the product cost of the systems in "Without Economizer" and "With Economizer" working modes variation with CO_2 condenser exit temperature, respectively.

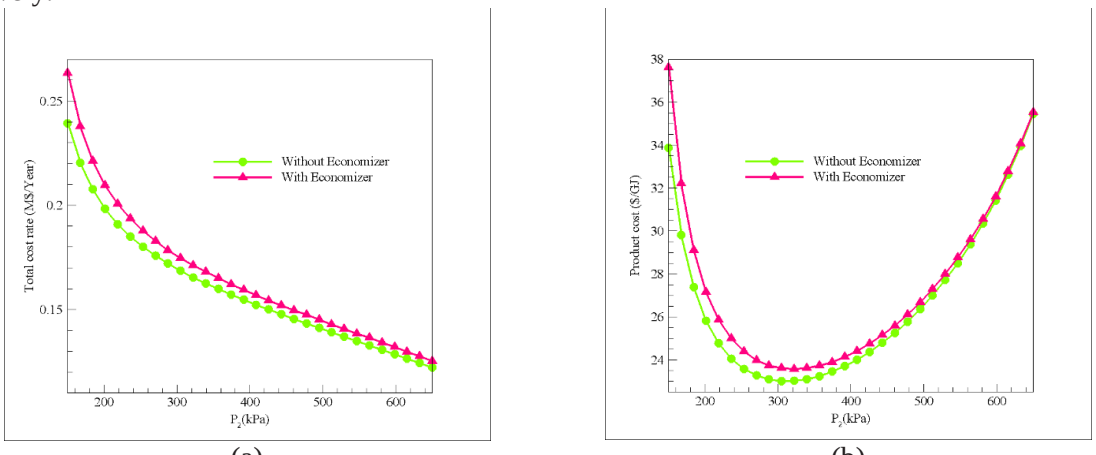

Fig. 5. (a) The total cost rate & (b) The product cost of the systems ("Without Economizer" and "With Economizer") variation with separator pressure.

The total cost rate decreases as the separator pressure increase from 150 to 650 kPa. This trend is sharp at first, and then the rate of decreasing slope decreases. Therefore, from the point of view of the total cost rate, increasing the separator pressure will have a positive effect on both systems. Regarding the production cost rate, different behavior is observed. As the separator

pressure increases from 150 kPa, the production cost rate values decrease steeply and reach a minimum of around 300 kPa. As the separator pressure increases from 300 kPa, both systems' production cost rate values start to increase. And this process continues up to a pressure of 650 kPa. Therefore, the best value of separator pressure for any system without an economizer is 23.01 $/GJ, which is obtained at a pressure of 305.2 kPa. For the system with an economizer, the best value is 23.57 $/GJ, which occurs at a pressure of 322.4 kPa. Figures 6(a) and (b) show the total cost rate and the product cost of the systems in "Without Economizer" and "With Economizer" working modes variation with CO_2 turbine inlet pressure, respectively. By increasing the turbine inlet pressure from 14000 kPa to 16000 kPa, both economic parameters under study have an increasing trend. As a result, increasing the inlet pressure of the carbon dioxide turbine, from an economic point of view, negatively affects both systems' performance. The noteworthy point in these graphs is that with the increase in pressure from 14000 kPa to 16000 kPa, the slope of the "without economizer" system is greater than the slope of the "with economizer" system, and the distance between the two lines gradually decreases.

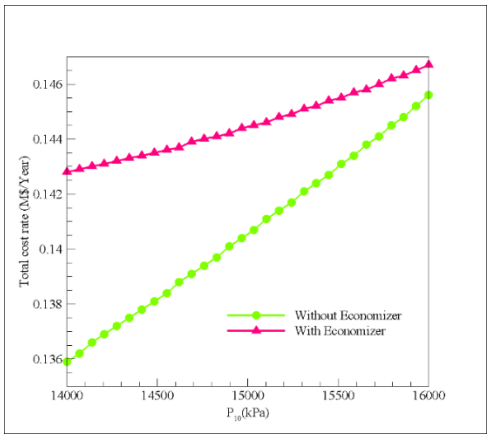

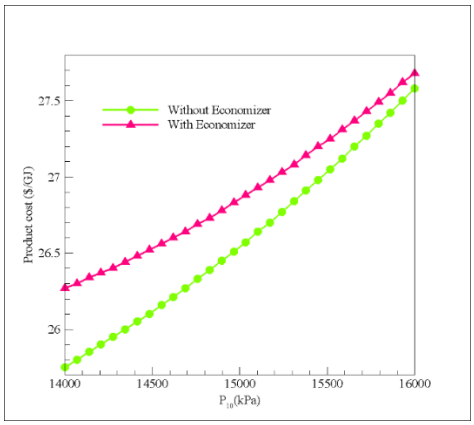

(a) (b)

Fig. 6. (a) The total cost rate & (b) The product cost of the systems ("Without Economizer" and "With Economizer") variation with CO2 turbine inlet pressure.

Figures 7(a) and (b) show the total cost rate and the product cost rate of the systems in "Without Economizer" and "With Economizer" working modes variation with CO_2 condenser exit temperature, respectively.

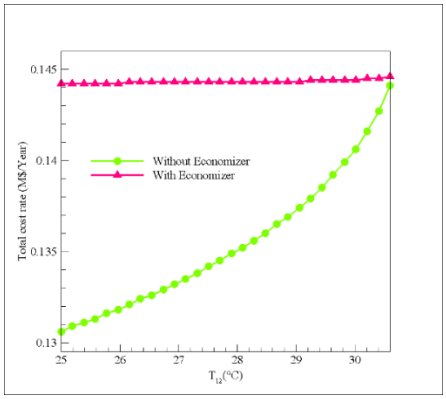

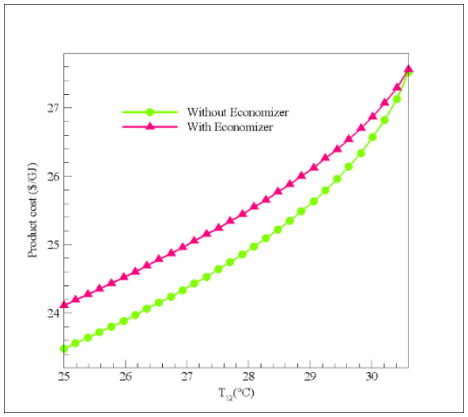

(a) (b)

Figure 7. (a) The total cost rate & (b) The product cost of the systems ("Without Economizer" and "With Economizer") variation with CO_2 condenser exit temperature.

By increasing the condenser output temperature from 25 °C to 31 °C, both economic parameters under study have an increasing trend. As a result, increasing the condenser output temperature, from an economic point of view, negatively affects both systems' performance. The noteworthy point in these graphs is that with the condenser output temperature from 25 °C to 31°C, the slope of the "without economizer" system is greater than the slope of the "with economizer" system, and the distance between the two lines gradually decreases. For future works, researchers should perform comparative economic and environmental analyses of the studied systems so that the effects of adding an economizer to the system can also be investigated from an economic and environmental point of view. In addition, advanced exergy analysis can also be a very significant idea for this study.

4. Conclusion

This study compares two operating modes of a single geothermal flash cycle, "without economizer" and "with economizer," both powered by a trans-critical carbon dioxide cycle. The primary objective is to investigate the impact of the economizer on various output parameters, including energy efficiency, exergy efficiency, and net power output. Based on the findings, the following conclusions can be drawn:

1. The "With Economizer" system exhibits an increase in net power output, rising from 389.2 kW to 401.3 kW, indicating a 3.1% improvement. According to the first law of thermodynamics, the energy efficiency also increases by 3.07%, with the "With Economizer" system achieving 6.53% compared to the 6.335% of the "Without Economizer" system. In terms of exergy efficiency, the "Without Economizer" system shows a value of 31.48%, while the "With Economizer" system achieves 32.46%, representing a 3.11% enhancement from the perspective of the second law of thermodynamics.
2. When the separator pressure ranges from 150 kPa to 650 kPa, both systems perform similarly. The graphs depicting energy efficiency, exergy efficiency, and net power output all exhibit an initial upward trend with increasing pressure until reaching a peak value of approximately 400 kPa. Subsequently, these parameters start to decline.
3. In the "Without Economizer" system, the three parameters (energy efficiency, exergy efficiency, and net power production) increase as the CO2 turbine's inlet pressure ascends from 13000 kPa to 17000 kPa, reaching a peak value at 15500 kPa. Beyond this point, these figures begin to decrease. However, the behavior differs in the "With Economizer" system, where all three parameters demonstrate a diminishing trend as the pressure rises from 13000 kPa to 17000 kPa, indicating the detrimental impact of raising the CO2 turbine's inlet pressure on the overall system performance.
4. All three graphs illustrate a declining trend as the temperature increases from 25 °C to 31 °C. This demonstrates the adverse effect of elevating the CO2 condenser exit temperature on the system's efficiency in both operating modes.
5. The total cost rate decreases as the separator pressure increases from 150 to 650 kPa. While the initial decline is steep, a gradual reduction follows. Consequently, raising the separator pressure benefits both systems in terms of the total cost rate. The manufacturing cost rate exhibits varied behavior, with a sharp decline in production cost rate values until reaching a minimum around 300 kPa of separator pressure. Beyond this point, the production cost rate for both systems increases as the separator pressure rises to 650 kPa.

Acknowledgement:

This work is supported by the National Natural Science Foundation of China (Grant Nos. 11972148). The authors extend their appreciation to King Saud University for funding this work through Researchers Supporting Project number (RSPD2023R711), King Saud University, Riyadh, Saudi Arabia. The authors are grateful to Eng. Raha Ranaei for providing some data for this research. This paper does not necessarily reflect the view of the funding agency.

Funding:

This research was funded by King Saud University through Researchers Supporting Project number (RSPD2023R711)"

References

[1] Wang, Y.-T., *et al.*, Estimation of shallow geothermal potential to meet heating demand in a building scale, *Thermal Science*, *27*. (2023), 1 Part B, pp. 607-614
[2] Zobaa, A.F.,R.C. Bansal, *Handbook of renewable energy technology*. World Scientific, 2011.
[3] Dong, Y., *et al.*, GEOTHERMAL CHARACTERISTICS OF THE XIANSHUIHE FAULT ZONE AND THEIR ENGINEERING INFLUENCE ON TUNNEL CONSTRUCTION, *Thermal Science*, *27*. (2023),
[4] Kurchania, A., *Biomass energy*, in: *Biomass Conversion*, (Ed., Editor^Editors), Springer. 2012, pp. 91-122.
[5] Nordin, N. *Limitations of Commercializing Fuel Cell Technologies*,AIP Conference Proceedings,2010,1225, pp. 498-506
[6] Zhang, L., Automatic storage of building thermal energy and heat pump heating based on wireless communication, *Thermal Science*, *27*. (2023), 2 Part A, pp. 1183-1190
[7] Karki, A.B., Biogas as renewable energy from organic waste, *Biotechnology*, *10*. (2009), pp. 1-9
[8] Huang, J., *et al.*, Exergy analyses and optimization of a single flash geothermal power plant combined with a trans-critical CO2 cycle using genetic algorithm and Nelder–Mead simplex method, *Geothermal Energy*, *11*. (2023), 1, p. 4
[9] Wang, H., *et al.*, Thermodynamic investigation of a single flash geothermal power plant powered by carbon dioxide transcritical recovery cycle, *Alexandria Engineering Journal*. (2023) Pages 441-450.
[10] Aryanfar, Y., *et al.*, Energy and exergy assessment and a competitive study of a two-stage ORC for recovering SFGC waste heat and LNG cold energy, *Energy*, *264*. (2023), p. 126191
[11] Liu, F., *et al.*, Comparative investigation on the heat extraction performance of an enhanced geothermal system with N2O, CO2 and H2O as working fluids, *Applied Thermal Engineering*, *200*. (2022), p. 117594
[12] Sahana, C., *et al.*, Integration of CO2 power and refrigeration cycles with a desalination unit to recover geothermal heat in an oilfield, *Applied Thermal Engineering*, *189*. (2021), p. 116744
[13] Wang, X., *et al.*, Working fluid selection for organic Rankine cycle power generation using hot produced supercritical CO2 from a geothermal reservoir, *Applied Thermal Engineering*, *149*. (2019), pp. 1287-1304
[14] Jiang, P.-X., *et al.*, Thermodynamic analysis of a solar–enhanced geothermal hybrid power plant using CO2 as working fluid, *Applied Thermal Engineering*, *116*. (2017), pp. 463-472
[15] Liu, Y., *et al.*, Thermodynamic comparison of CO2 power cycles and their compression processes, *Case Studies in Thermal Engineering*, *21*. (2020), p. 100712
[16] Cao, Y., *et al.*, Study and multi-objective optimization of integrating an energetic solar thermal application, a supercritical process, and a high-temperature electrolyser, *Case Studies in Thermal Engineering*, *40*. (2022), p. 102530
[17] Liu, X., *et al.*, Conventional and advanced exergy analyses of transcritical CO2 ejector refrigeration system equipped with thermoelectric subcooler, *Energy Reports*, *7*. (2021), pp. 1765-1779

[18] Parikhani, T., *et al.*, Performance enhancement and multi-objective optimization of a double-flash binary geothermal power plant, *Energy Nexus*, *2*. (2021), p. 100012
[19] Melzi, B., *et al.*, Modelling and Optimal Design of Hybrid Power System Photovoltaic/Solid Oxide Fuel Cell for a Mediterranean City, *Energy Engineering*, *118*. (2021)
[20] Yazarlou, T.,M.D. Saghafi, Investigation of Plans Shape and Glazing Percentage for the Energy Efficiency of Residential Buildings, *Energy Engineering*, *118*. (2021)
[21] Pambudi, N.A., *et al.*, Experimental Investigation of Organic Rankine Cycle (ORC) for Low Temperature Geothermal Fluid: Effect of Pump Rotation and R-134 Working Fluid in Scroll-Expander, *Energy Engineering*, *118*. (2021), 5
[22] Saengsikhiao, P., *et al.*, Development of Environmentally Friendly and Energy Efficient Refrigerants for Refrigeration Systems, *Energy Engineering*, *118*. (2021)
[23] Wang, J., *et al.*, Thermodynamic analysis and optimization of a flash-binary geothermal power generation system, *Geothermics*, *55*. (2015), pp. 69-77
[24] Chen, L., *et al.*, Energy and exergy analysis of two modified adiabatic compressed air energy storage (A-CAES) system for cogeneration of power and cooling on the base of volatile fluid, *Journal of Energy Storage*, *42*. (2021), p. 103009
[25] Mohtaram, S., *et al.*, Energy-exergy efficiencies analyses of a waste-to-power generation system combined with an ammonia-water dilution Rankine cycle, *Case Studies in Thermal Engineering*, *25*. (2021), p. 100909
[26] Peng, W., *et al.*, Enhancement technology of underground water flow field in coal mine to improve energy efficiency of heat pump system in geothermal energy development, *Thermal Science*, *27*. (2023), 2 Part A, pp. 1191-1198
[27] Aali, A., *et al.*, Exergoeconomic analysis and multi-objective optimization of a novel combined flash-binary cycle for Sabalan geothermal power plant in Iran, *Energy Conversion and Management*, *143*. (2017), pp. 377-390
[28] El Haj Assad, M., *et al.*, Energy, exergy, economic and exergoenvironmental analyses of transcritical CO2 cycle powered by single flash geothermal power plant, *International Journal of Low-Carbon Technologies*, *16*. (2021), 4, pp. 1504-1518
[29] Sun, H., *et al.*, An Energy Efficiency Improvement Method for Manufacturing Process Based on ECRSR, *Energy Engineering*, *117*. (2020), 3
[30] Xue, Y., *et al.*, Heat management system of electric vehicle based on heat pump and energy recovery of removable battery, *Thermal Science*, *27*. (2023), 2 Part A, pp. 1215-1221
[31] Rasheed, M., *et al.*, Decision-making algorithm based on Pythagorean fuzzy environment with probabilistic hesitant fuzzy set and Choquet integral, *AIMS Mathematics*, *8*. (2023), 5, pp. 12422-12455
[32] Hadi, F., *et al.*, NUMERICAL SOLUTIONS OF NONLINEAR DELAY INTEGRO-DIFFERENTIAL EQUATIONS USING HAAR WAVELET COLLOCATION METHOD, *Fractals*, *31*. (2023), 02, p. 2340039
[33] Raouf, A., *et al.* (2023) *Wind Energy Conversion Systems Based on a Synchronous Generator: Comparative Review of Control Methods and Performance*. Energies 16
[34] Mosaffa, A.H., *et al.*, Thermo-economic analysis of combined different ORCs geothermal power plants and LNG cold energy, *Geothermics*, *65*. (2017), pp. 113-125
[35] Bejan, A., *et al.*, *Thermal design and optimization*. John Wiley & Sons, 1995.
[36] Huang, D., *et al.*, Evaluation of thermal performance of air source heat pump heating system based on electricity equivalent, *Thermal Science*. (2022), 00, pp. 6-6
[37] Baghernejad, A.,M. Yaghoubi, Exergoeconomic analysis and optimization of an Integrated Solar Combined Cycle System (ISCCS) using genetic algorithm, *Energy Conversion and Management*, *52*. (2011), 5, pp. 2193-2203
[38] Xu, G., *et al.* (2014) *An Improved CO2 Separation and Purification System Based on Cryogenic Separation and Distillation Theory*. Energies 7, 3484-3502
[39] Ji, X., *et al.*, Technical requirements analysis of integrated paralleled-loop exhaust air heat pump system applied to ultra-low energy building in different climatic regions of China, *Thermal Science*, *26*. (2022), 5 Part A, pp. 3911-3922

Submitted: 3.05.2023.
Revised: 24.06.2023
Accepted: 28.06.2023.